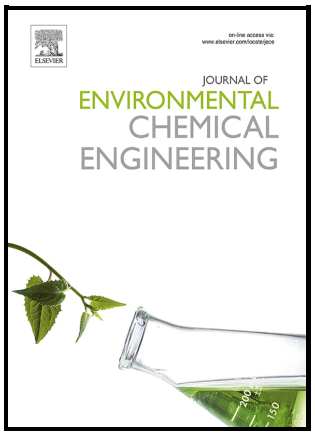

Stability of a Feed-Effluent Heat Exchanger / Reactor system for catalytic combustion of VOCs: Influence of variable emission patterns

Ángel Miranda, María Rodríguez, Luis Cadús, Daniel Borio

PII: S2213-3437(21)00574-1

DOI: https://doi.org/10.1016/j.jece.2021.105597

Reference: JECE105597

To appear in: *Journal of Environmental Chemical Engineering*

Received date: 25 January 2021
Revised date: 20 April 2021
Accepted date: 23 April 2021

Please cite this article as: Ángel Miranda, María Rodríguez, Luis Cadús and Daniel Borio, Stability of a Feed-Effluent Heat Exchanger / Reactor system for catalytic combustion of VOCs: Influence of variable emission patterns, *Journal of Environmental Chemical Engineering,* (2021) doi:https://doi.org/10.1016/j.jece.2021.105597

Stability of a Feed-Effluent Heat Exchanger / Reactor system for catalytic combustion of VOCs: Influence of variable emission patterns

Miranda, Ángel[1], Rodríguez, María[2*], Cadús, Luis[2], Borio, Daniel[1]

1 Planta Piloto de Ingeniería Química (PLAPIQUI-UNS/CONICET) Camino La Carrindanga km. 7, 8000, Bahía Blanca, Argentina.

2 Instituto de Investigación en Tecnología Química (INTEQUI-UNSL/CONICET), Almte. Brown 1455, 5700 San Luis, Argentina.

**E-mail:* mlrodri@unsl.edu.ar

Abstract

In this contribution, a theoretical study of the dynamic behaviour (open- and closed-loop) of a Feed-Effluent Heat Exchanger (FEHE) / Reactor system for the catalytic combustion of Volatile Organic Compounds (VOCs) is carried out. An additional supply of energy is provided by means of a furnace to achieve the desired reactor inlet temperature. The positive feedback of energy to the reactor inlet is a source of instability that leads to pronounced limit cycles in the main state variables. The strong thermal oscillations predicted can damage the catalyst and cause considerable stress on both the reactor and heat exchanger materials. To prevent this scenario, a control structure that considers the manipulation of a bypass flow of the feed stream around the FEHE is selected. A single-loop feedback control system is successfully applied to maintain the inlet temperature set-point, rejecting the VOC's concentration disturbances and enabling a stable operation. The results demonstrate that the controllability of the process is ensured with high external heat supplies (low heat recovery in the FEHE) which increases the fuel demand and the operating costs. Additionally, a high FEHE transfer area enables efficient heat recovery and avoids the controllability loss due to a suitable by-pass valve regulation.

Graphical abstract

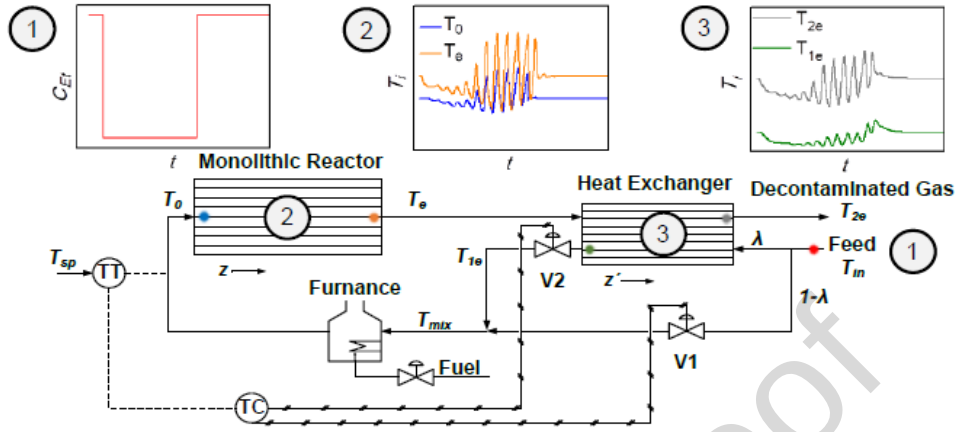

Keywords

VOC; catalytic oxidation; reactor; Feed-Effluent Heat Exchanger.

1. Introduction

The success of monoliths as engine emission converters has encouraged researchers to use monolithic reactors for stationary applications [1]. Catalytic ozone conversion [2], selective catalytic NOx reduction [3] and catalytic VOCs combustion are representative examples. In this last process, high volumes of air characterized by a very low concentration of organic species must be preheated up to the light-on temperature to enhance the combustion reaction in order to achieve a decontaminated gas stream. An Emission Limit Value of carbon (ELV) of 20 mg C/Nm^3 (milligrams of carbon per normal cubic meter) for streams discharged into the atmosphere has been stated by the European Commission [6].

Practically, most industrial emissions are less than 10000 m^3/h flowrate with VOCs concentration between 50 and 2000 ppm [4, 5]. It is very important to reduce the energy demand in the treatment of high flow rates by heat recovery because this process is an end-line process.

A common industrial configuration for this purpose is the recuperative catalytic oxidation: VOCs emission stream is first preheated by a heat-exchanger, where its temperature can increase by approximately 50–200 °C; the afterward furnace will further heat the feed stream to the light-off reaction temperature, and then the VOCs oxidation is boosted to produce CO_2 and H_2O with considerable heat release. The energy efficiency of this process is generally lower than 70%, which means it requires

additional energy to maintain the equipment working on VOCs removal [5]. According to some authors recuperative catalytic oxidation is not appropriate to deal with large-volume and low-concentration VOCs pollution [7,8]. However, taking into account the low initial investment and high flexibility, the recuperative catalytic oxidation is rather suitable for small flowrates (<5000 m^3/h) VOCs pollution cases. According to the discussion above, catalysts with out-standing low-temperature activity are pivotal for the engineering application of VOCs removal [5].

Feed-effluent heat exchangers (FEHEs) are widely used in high-temperature exothermic adiabatic tubular reactor systems to conserve energy [9, 10]. Previous research has shown the tendency of these systems to either quench ("blowout" or "extinguish" to a low-temperature steady state) or runaway ("blowup" to a high-temperature steady state). Also, they can exhibit open-loop instability as a result of the positive feedback of energy from the preheating system to the reactor [9]. Bildea and Dimian [11] studied the steady-state and dynamic behaviour of a heat-integrated PFR, consisting of a FEHE, a furnace, an adiabatic tubular reactor, and a steam generator. The system exhibits oscillatory behaviour for realistic values of the model parameters. The selection of the FEHE efficiency is a critical step to achieve the desired state multiplicity and to ensure stability. Morud and Skogestad [12] showed that an industrial ammonia reactor coupled with a FEHE could reach limit cycles due to the sustained oscillation of the process variables over time.

Several control structures have been proposed to control the reactor inlet temperature. Silverstein and Shinnar [13] studied the effects of design parameters on the dynamic stability of systems with a FEHE followed by a furnace before the adiabatic reactor. They recommended controlling the reactor inlet temperature with the furnace duty. They also explored bypassing of cold material around the FEHE to provide an additional manipulated variable. Terrill and Douglas [14] examined in the HDA process the use of multiple FEHEs in series to preheat the reactor feed with hot reactor effluent. In the process, a furnace is located before the reactor.

Among the most common control structures, it is suggested the control of the temperature of the mixed stream after the FEHE by manipulating the bypass flow and controlling the reactor inlet temperature by manipulating fuel to the furnace [9]. If, in the case of total closure of the by-pass valve, the temperature rise in the FEHE is not sufficient, the fuel flow to the furnace could be manipulated for additional energy supply. It is important to note that in industrial processes, VOCs catalytic oxidation

often operates under variable emission patterns: feed VOCs concentration can fluctuate within wide ranges. In the case of high feed VOCs concentrations, the heat released in the combustion reactions favours VOCs abatement. Conversely, for low feed concentrations, auxiliary fuel requirements for preheating can be substantial, increasing the operating costs. In all the cases, the inlet temperature set point should be high enough to prevent VOCs emissions. In order to minimize the heat supply, it is convenient to maintain the reactor inlet temperature at a minimum value ($T_{0,min}$) [15], which guarantees the complete VOCs abatement, even in the case of significant changes in the VOCs concentration of the feed stream [16].

Another aspect to take into account in this system is the inverse responses typical of reactor dynamics [9]. In particular, reactors with a severe inverse response are difficult to control when coupled with a heat exchanger [17].

Implementing an effective control strategy in this complex scenario is a major challenge that has not been done before for catalytic VOC combustion.

Understanding the dynamic behaviour of the process and the control system is crucial to i) minimize out-of-specification times (ELV not fulfilled), ii) avoid oversizing of main equipment and reduce investment costs, iii) minimize operating costs due to external heat supply and iv) avoid severe thermal oscillations that can damage the catalyst and cause considerable stress on both the reactor and heat exchanger materials.

In the present work, a FEHE/Reactor system for the VOCs catalytic combustion process is studied. In Section 2 the mass and energy conservation equations of a non-isothermal pseudo homogeneous 1-D model are presented together with a description of the numerical solution method. Section 3 **(**Results and discussion**)** includes an open-loop analysis to understand the stability of the main operative variables, the selection/implementation of a control strategy to perform a stable process, a closed-loop study under changes in the reactor inlet temperature set point and inlet VOC concentration. Finally, it is included an exploration of the influence of the heat exchanger area to achieve efficient and stable system control. Section 4 summarizes the main conclusions.

2. Mathematical model

2.1. Model equations

Figure 1 shows the schematic representation of the process under study. A monolithic reactor is coupled with an upstream Feed-Effluent Heat Exchanger and a natural gas

furnace to complete the feed preheating. The cold fresh feed, a stream of ethanol diluted in air, enters the FEHE (a gas-gas plate heat exchanger) and is heated by the hot stream of the decontaminated gas leaving the exothermic reactor. A portion of the cold feed is bypassed around the FEHE and mixed with the hot exit stream. The additional heat required to achieve the desired reactor inlet temperature is supplied by the furnace.

For the closed–loop analysis, a single-loop feedback control system is selected to maintain the temperature set point at the reactor inlet (T_0) by handling the bypass valve. Since the reactor inlet temperature is controlled by manipulating the bypass flow, not the fuel to the furnace [9], a constant value of the heat duty in the furnace is assumed. In practice, there are control valves both in the line through the FEHE and the bypass line, with the aim of achieving the required fluid mechanics [18].

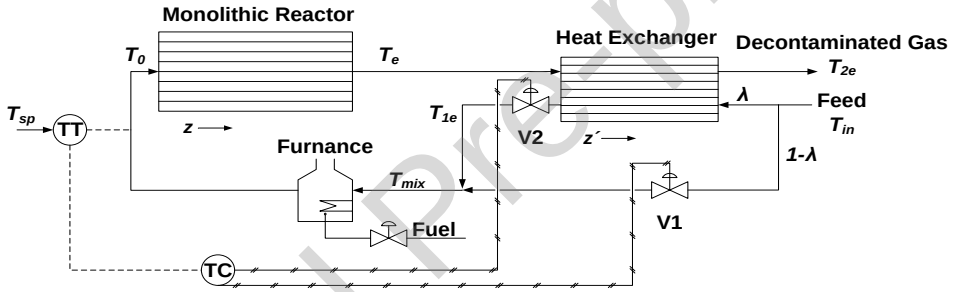

Fig.1. Schematic representation of the reactor/FEHE/furnace process.

The ceramic monolithic reactor of square section channels is considered as perfectly insulated. The channel's walls are impregnated with a Mn–Cu mixed oxide catalyst [19].

The catalytic combustion of ethanol for this catalyst is evaluated using the kinetic model proposed by Campesi et al. [20]. LHHW (Langmuir-Hinshelwood-Hougen-Watson) expressions were proposed for the system of the reactions involved: partial oxidation of ethanol to acetaldehyde (reaction 1) and combustion of acetaldehyde (reaction 2, see Table 1). LHHW contains a denominator that represents the reduction in the rate due to the adsorption phenomena. Its individual terms represent the distribution of the active sites among the possible surface complexes and vacancies, in this system of reactions acetaldehyde is the main adsorbed species. Table 2 lists the effective kinetic parameters [21] and the standard heats of reactions 1 and 2.

Table 1. Reaction system and kinetic expressions [20]

Reaction System	Kinetic expression	
$C_2H_6O + (1/2)O_2 \rightarrow C_2H_4O + H_2O$	$r_1 = \frac{k_{ref1}\exp\left[-(E_1/R)(1/T - 1/T_{ref})\right]C_{Et}}{1 + Kc_{Et}C_{Et} + Kc_{Ac}C_{Ac}}$	(1)
$C_2H_4O + (5/2)O_2 \rightarrow 2CO_2 + 2H_2O$	$r_2 = \frac{k_{ref2}\exp\left[-(E_2/R)(1/T - 1/T_{ref})\right]Kc_{Ac}C_{Ac}}{1 + Kc_{Et}C_{Et} + Kc_{Ac}C_{Ac}}$	(2)

Table 2. Effective kinetic parameters and standard heats of reaction [21].

Parameter	Value
$k_{ref,1}$	1.71×10^3 s^{-1}
$k_{ref,2}$	1.8×10^{-1} mol s^{-1} m^{-3}
E_1	1.1124×10^5 J mol^{-1}
E_2	1.62×10^5 J mol^{-1}
Kc_{Ac}	6.75×10^2m^3 mol^{-1}
Kc_{Et}	~0
$-\Delta H^0_{r1}$	1.73 x 10^5 J/mol
$-\Delta H^0_{r2}$	1.10 x 10^6 J/mol

A pseudohomogeneous 1D model is proposed to simulate the non-steady state operation of the monolith reactor, based on the following hypotheses:

(a) Fully developed laminar flow through the channels is assumed leading to low pressure drops

(b) Adiabatic and isobaric conditions are assumed.

(c) Concentration and temperature variations in the transverse direction are neglected [22].

(d) Plug flow is assumed inside the channels.

(e) Axial dispersion of heat and mass is neglected (axial mass and heat Peclet numbers are much higher than 50) [22].

(f) Internal mass transfer diffusional limitations and external mass and heat resistances are considered by means of an effective reaction kinetics (see Table 2).

(g) A single channel is representative of the entire reactor.

By assuming that the distribution of the washcoat is uniform around the perimeter of the cell, the catalyst layer may then be modelled as a slab of thickness δ_w.

Since there are two reactions involved, mass balances corresponding to ethanol and acetaldehyde are included to calculate the extents of reaction 1 (ε_1) and 2 (ε_2). The concentrations of the remaining species CO_2, O_2, N_2, and H_2O are obtained from the stoichiometry as a function of the parameters ε_{1r} and ε_{2r} [23].

Under the stated hypotheses, the process is represented by the following equations:

Reactor balances

Mass balances

$$\frac{\partial C_{Et}}{\partial t} = -\frac{1}{\tau_{MB}}\left[\frac{\partial C_{Et}}{\partial z} - \frac{r_1^{eff}}{u_s}\right] \tag{3}$$

$$\frac{\partial C_{Ac}}{\partial t} = -\frac{1}{\tau_{MB}}\left[\frac{\partial C_{Ac}}{\partial z} + \frac{\left(r_1^{eff} - r_2^{eff}\right)}{u_s}\right] \tag{4}$$

Where:

$$\tau_{MB} = \frac{\varepsilon}{u_s} \tag{5}$$

Heat balance

$$\frac{\partial T}{\partial t} = \frac{1}{\tau_{HB}}\left[-\frac{\partial T}{\partial z} + \frac{\left(r_1^{eff}(-\Delta H_1) + r_2^{eff}(-\Delta H_2)\right)A_t}{\dot{m}_g Cp_g}\right] \tag{6}$$

Where:

$$\tau_{HB} = \frac{\left(A_s \rho_s Cp_s + A_w \rho_w Cp_w\right)}{\dot{m}_g Cp_g} \tag{7}$$

Inlet conditions

At z=0: $C_{Et} = C_{0Et}; C_{Ac} = C_{0Ac}; T = T_0$ (8)

Initial conditions

At t=0: $C_{Et}(z) = C_{Et}^{SS}; C_{Ac}(z) = C_{Ac}^{SS}; T(z) = T^{SS}$ (9)

FEHE heat balances

Cold stream (1)

$$\frac{\partial T_1}{\partial t} = \frac{1}{\tau_1}\left[\frac{\partial T_1}{\partial z'} + \frac{2b'U}{u_1\bar{\rho}_1\overline{Cp}_1 A_f'}\left(T_2 - T_1\right)\right] \tag{10}$$

Hot stream (2)

$$\frac{\partial T_2}{\partial t} = \frac{1}{\tau_2}\left[-\frac{\partial T_2}{\partial z'} - \frac{2b'U}{u_2\bar{\rho}_2\overline{Cp}_2 A_f'}\left(T_2 - T_1\right)\right] \tag{11}$$

Where:

$$\tau_1 = \frac{A'\rho' Cp'}{u_1\bar{\rho}_1\overline{Cp}_1 A_f'} \tag{12}$$

$$\tau_2 = \frac{A'\rho' Cp'}{u_2\bar{\rho}_2\overline{Cp}_2 A_f'} \tag{13}$$

Overall heat transfer coefficient, *U*:

$$\frac{1}{U} = \frac{1}{h_1} + \frac{\delta'}{k'} + \frac{1}{h_2} \tag{14}$$

$$h_k = \frac{k_k Nu_k}{HD} \tag{15}$$

for k =1,2

$$Nu_i = C\left(1 + B\,\mathrm{Re}\,\mathrm{Pr}\,\frac{HD}{L}\right)^{0.45} \tag{16}$$

The convective heat transfer coefficients are obtained from the Nusselt expression where *C* and *B* take values corresponding to the geometry of the plate [22].

Boundary conditions

$$T_1(z' = L') = T_{1in}\,; T_2(z' = 0) = T(z = L) \tag{17}$$

Initial conditions

At t=0: $T_1(z') = T_1^{SS}(z')_{;}\, T_2(z') = T_2^{SS}(z')$ (18)

An instantaneous dynamic for the mixer and the furnace after the FEHE is considered.

Mixer heat balance

$$T_{mix} = T_{1in} + \lambda\frac{\overline{cp}_{1e}\left(T_{1e} - T_{1in}\right)}{\overline{cp}_{mix}} \tag{19}$$

Furnace heat balance

$$T_0 = T_{mix} + \frac{\dot{Q}_F}{\overline{cp}_{mix}\,\dot{m}} \tag{20}$$

Controller

$$(1-\lambda) = \overline{(1-\lambda)} + K_c\left(er + \frac{1}{\tau_I}\int_0^t er\,dt\right) \tag{21}$$

The operating conditions assumed in the simulations are listed in Table 3. The geometrical parameter of the reactor and the heat exchanger are listed in Table 4.

Table 3. Process operating conditions.

Parameter	Value
Inlet VOC concentration, C_{0Et}	0 – 600 mg C/Nm^3
Volumetric feed flow rate, F_{v0}	61 m^3/hr
Pressure, P	101.325 kPa
Inlet temperature, $T_{1,In}$	20°C
Set point temperature, T_{sp}	179 °C – 185 °C
Gas-hourly space velocity (at the reactor), *GHSV*	1.745x10^4 1/h
By-pass ratio, λ	0.63 - 0.90
Furnace heat flow, Q_F	300 – 600 W

Table 4. Geometrical parameters.

Parameter	Value
Reactor	
Channel length, L	0.2 m
Channel width= height, b	1115 µm
Cell density	400 cpsi
Channels number, CN	13924
Monolithic material	Cordierite ($2MgO\text{-}2Al_2O_3\text{-}5SiO_2$)
Catalytic material	Mn-Cu

Average washcoat thickness	20 µm
Washcoat density, ρ_w	4030 kg/m^3
Washcoat mass, m_w	980 g
Heat exchanger	
Type/ flow configuration	Plates / Countercurrent
Plate length, $L´$	0.16m
Plate width, $b´$	0.08m
Channel height, δ_{HE}	1 mm
Plate thickness, δ_p	0.4 mm
Plates number, PN	70
Heat exchanger material	Stainless steel (AISI 316)

The parameters of the controller are listed in Table 5.1

Table 5. Parameters PI Controller

Controller parameter	Value
Proportional action parameter, K_C	0.003
Integral action parameter, τ_I	0.5

2.2. Numerical solution

The steady-state model of the FEHE / Reactor system constitutes a Boundary Value Problem, which is solved by discretizing the axial coordinate and using the Broyden Method.

The dynamic model is solved by discretizing the axial coordinate in the reactor and the FEHE (eqs. 3, 4, 6, 10, 11), using finite differences. Integration in time was performed by means of a Gear Algorithm [24].

3. Results and discussion

Figure 2 shows the axial temperature profiles along the monolithic reactor and the counter-current plate heat exchanger for a base case. The temperature downstream of the mixer (T_{mix}) and the temperature rise caused by the furnace (ΔT_F) are also indicated. The reactor inlet temperature (T_0 = 185 °C) is controlled through a by-pass valve (V1) and a downstream FEHE valve (V2) to regulate the flows around and through the heat

exchanger, respectively. For the base case, 36.6 % of the feed stream is bypassed around the FEHE, i.e. the selected value of λ is 0.634. The preheated feed (λF_T) is then mixed with the by-pass stream $(1 - \lambda)F_T$ at T_{1in} = 20°C. At the mixer, the temperature reaches 140 °C. Inside the furnace, the mixed stream receives a constant external heat supply (Q_F = 600 W), which increases their temperature to 185 °C.

The nested figure shows axial concentration profiles of ethanol, acetaldehyde (intermediary VOC compound) and total volatile organic compounds. It is observed that for the base case VOCs are completely consumed around 75 % of the reactor length.

The axial temperature profile inside the reactor is on the rise, showing a sharper increase when acetaldehyde is consumed, because the second reaction is more exothermic (see ΔH_{r2} in Table 2). When VOCs are consumed and both reactions are fully extinguished, the axial temperature profile reaches a plateau, this final temperature corresponds to the adiabatic temperature rise (ΔT_{ad}), which is proportional to the VOC concentration in the feed stream. In the base case, the catalytic combustion of 600 mg C/Nm^3 of ethanol leads to a total temperature rise of 27 °C. As VOCs concentration increases, the reactor outlet stream temperature becomes hotter.

For the analysed case, the energy of the reactor effluent is 8.9 10^3 kJ/h from which 62% (5. 5 10^3 kJ/h) is recovered in the heat exchanger, minimizing the external heat supply.

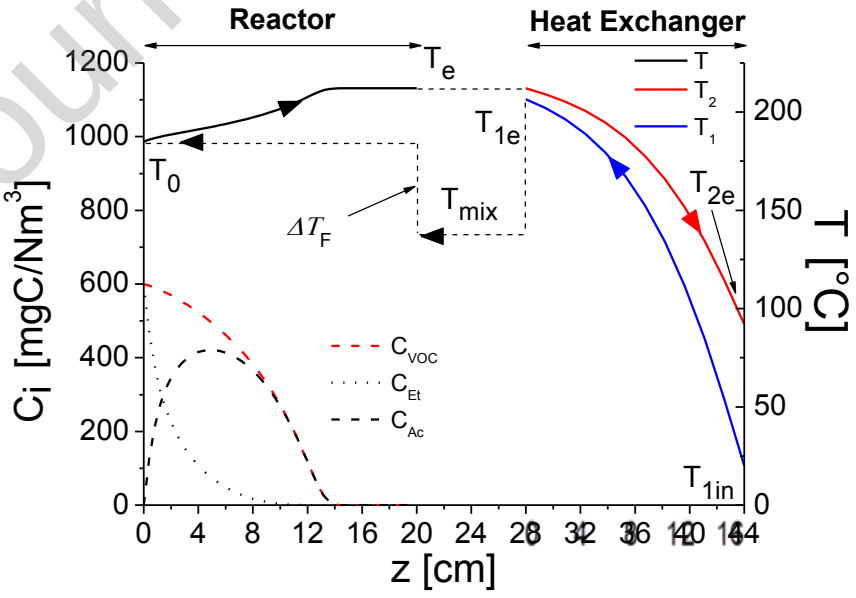

Fig. 2. Axial temperature profile and axial concentrations *profile* T_0=185°C, C_{0Et}= 600 mg C/Nm^3, T_{1in}= 20°C, F_{V0}= 61 m^3/h, Q_F= 600 W (ΔT_F = 45 °C)

3.1. Open Loop Analysis

In this section, the open-loop process dynamic is studied in the absence of disturbances, considering a constant heat supply in the furnace.

Figure 3a) presents the temporal profiles of both the reactor inlet temperature (T_0) and the reactor outlet temperature (T_e); Figure 3b) shows the temporal profiles of the heat-exchanger outlet temperatures (T_{1e} and T_{2e}) and, Figure 3c) exhibits the temporal VOC concentration profiles at three axial position inside the reactor, z= 0, 10 and 20 cm.

It is noticed a sustained oscillatory dynamic in the temperature profiles and also in the VOC concentration profile at z = 10 cm, as a result of the positive heat feedback to the reactor inlet. At z = 0 the VOC concentration is constant (feed concentration) and at z = 20 cm VOC concentration is zero (total VOC consumption), and both remain invariant in time. The oscillatory behaviour of the reactor temperature is in accordance with that reported in the open literature for other processes [11, 12].

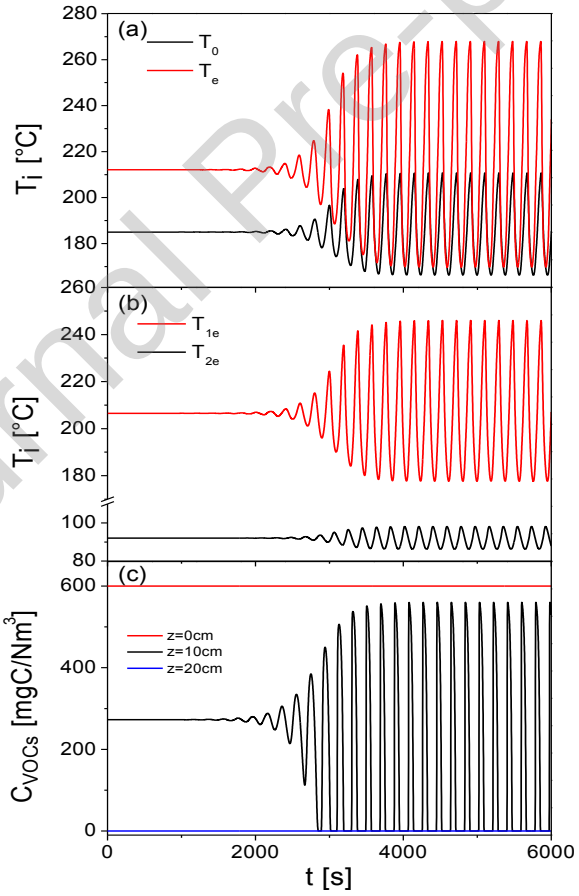

Fig. 3. (a) Temporal profiles of the reactor inlet and outlet temperatures. (b) Temporal profiles of heat exchanger outlet temperatures (streams 1 and 2) and (c) Temporal profiles of VOCs concentration at different positions (z= 0, 10, 20 cm), at the conditions of Figure 2.

The sustained oscillations originate the limit cycle shown in Figure 4, where the reactor outlet temperature is represented against the reactor inlet temperature. The centre dot shows the initial process condition (T_0 =185 °C; T_e= 212.1 °C). The process moves in a spiral path to the limit cycle that corresponds to the sustained oscillatory (or marginally stable) temporal profile.

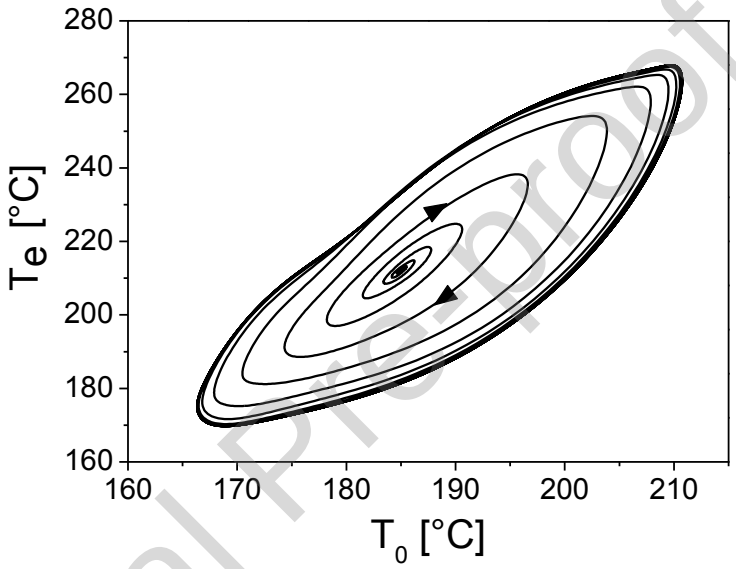

Fig. 4. Limit cycle of the process for C_{0Et}= 600 mg C/Nm^3, T_{1in}= 20 °C, F_{V0}= 61 m^3/h, Q_F= 600 W. Initial Steady State (t= 0 s): T_0= 185 °C and T_e= 212.12 °C

Figure 5 exhibits the limit cycles of the system for different external heat supply (Q_F= 220, 600, 1000 and 1400 W). Despite the different external heat supplies, the same initial condition is achieved in the reactor. This common steady-state point is shown in the figure as a red dot called *Initial Steady State*. Table 6 lists the heat supply policies selected in each case to provide a total heat duty of 2150 W.

It is observed that at higher heat external supplies (lower heat recovery in the FEHE), the limit cycle tends to decrease. As a consequence, the time profiles of the reactor inlet temperature show lower amplitude oscillations, which begin considerably later (see Figure 6). When the total heat duty is provided by the external source, the limit cycle disappears and a stable operation is achieved. The heat supply of the furnace provides a clear stabilizer effect [9].

It is also observed in Figure 5 that a section of the cycles of Q_F =220 W and Q_F= 600 W is below the identity line (T_0 = T_e), which means that the outlet temperature becomes lower than the inlet temperature of the reactor in these periods of time.

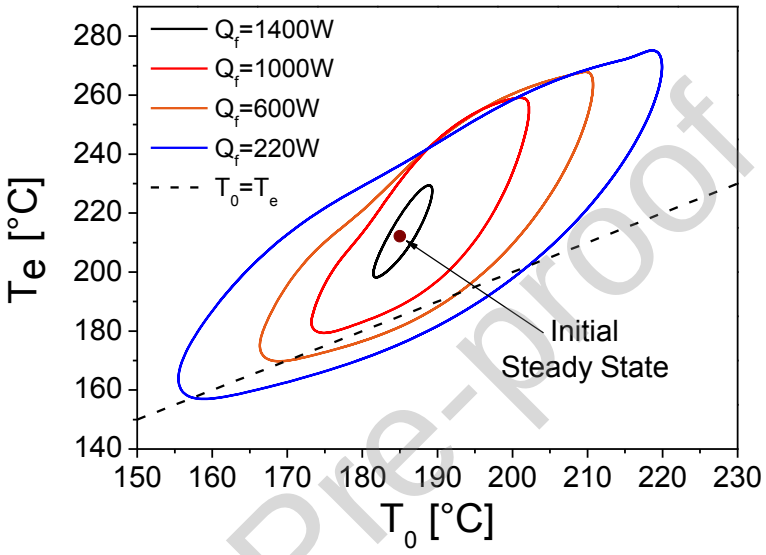

Fig 5. Limit cycle of the process for different heat supply from the furnace (Q_F= 220, 600, 1000 and 1400 W) for the condition of Fig 2.

Table 6. Furnace heat and recovery heat to maintain T_0= 185 °C (constant)

Q_F (W)	Q_R (W)	Q_{tot} (W)
220	1930	2150
600	1550	2150
1000	1150	2150
1400	750	2150

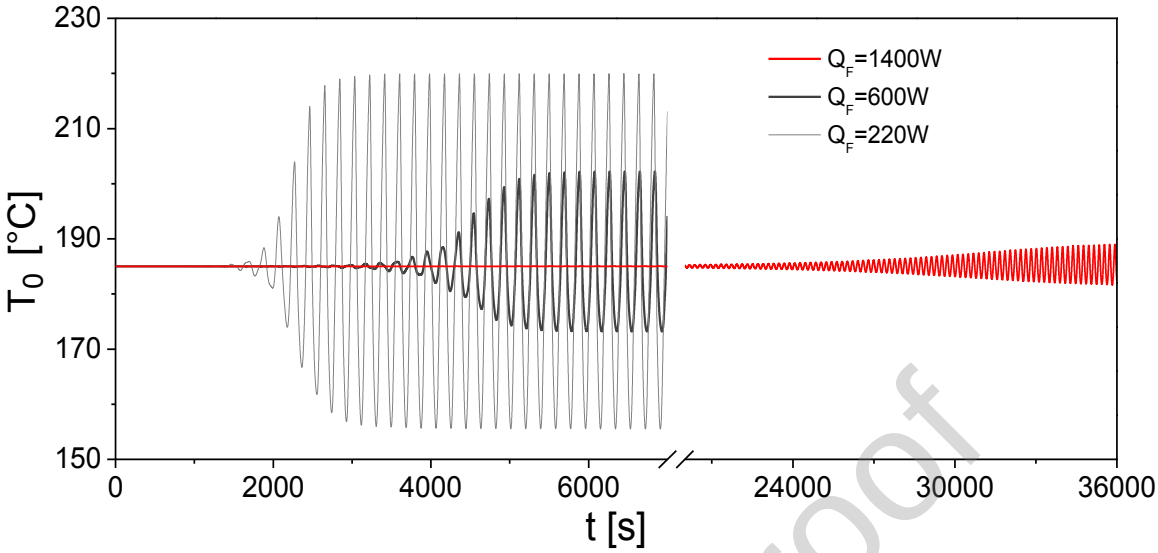

Fig. 6. Temporary profiles of the reactor inlet temperature for different furnace heat supply (Q_F= 220, 600 and 1400 W)

3.2. Closed Loop Analysis

3.2.1. Influence of the reactor inlet temperature set point ($T_{0,SP}$)

Figure 7 shows the dynamic response of the process against a decrease from 185 °C to 182 °C in the inlet temperature set point $T_{0,SP}$ (negative step).

The reactor outlet temperature profile (T_e) exhibits a sharp increase (~12 °C) as a consequence of the decrease of 3 °C in T_0, reaching a maximum temperature of 225 °C, at t= 150 s. This inverse response or wrong-way behaviours is typical of reactor dynamic and it has been extensively studied [9, 12, 25]. Finally, the outlet temperature drops below its initial value as expected.

As a result of the process configuration, the outlet temperature of the cold stream in the FEHE (T_{1e}) presents an analogous behaviour to that of T_e.

The fraction of stream through the FEHE (λ) shows an instantaneous drop due to the set point change for accomplishing the new $T_{0,SP}$. Then, as a consequence of the maximum observed in T_e, λ presents a momentaneous diminution (less flowrate preheated to high temperature). After that, λ reaches a new steady-state value (0.625) lower than the initial one (0.634) and higher than the initial drop (0.61). This is the result of two conditions: at first, the heat duty diminishes but T_e is high, and a lower flow rate is required through the FEHE, then, when the system evolves to a new steady-state, the final T_e is 3 °C lower than the initial and, λ is stabilized in a value higher than the first drop but lower than the value at t= 0 s.

In this operating condition, the VOCs abatement over time is complete, and stable and efficient process control is achieved. To maintain controllability conditions in the by-pass valve, the variable λ is allowed to vary between the range λ= 0.1 (valve almost fully open) and λ= 0.9 (valve almost fully closed).

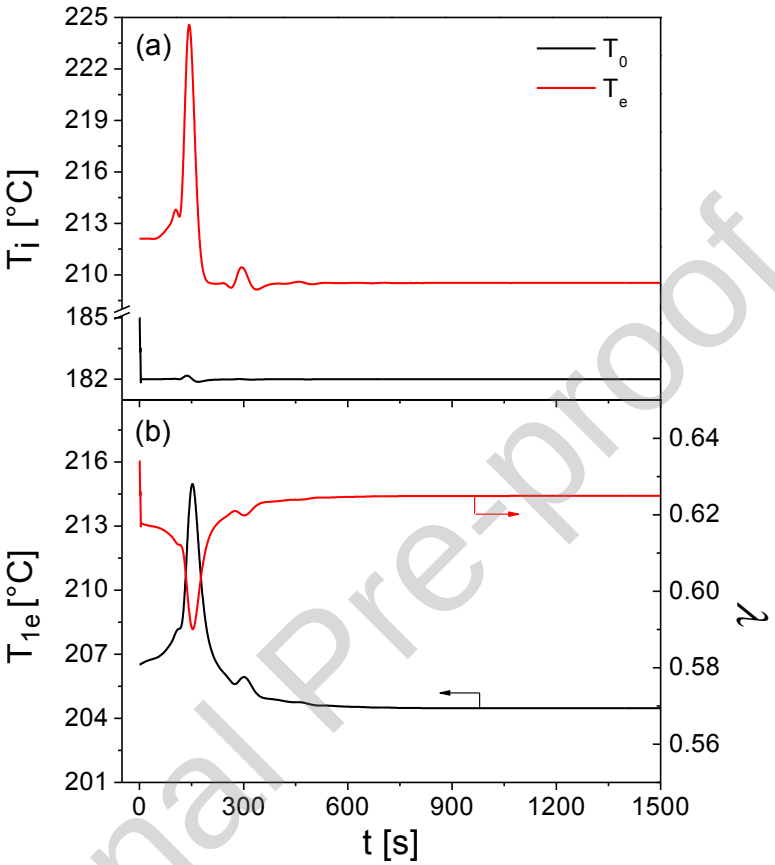

Fig. 7. (a) Temporary profiles of the reactor inlet and outlet temperatures, and (b) temporary profile of the heat exchanger outlet temperature (T_{1e}) and temporary profile of the ratio of flow rate through FEHE, for a negative step in $T_{0,SP}$ from 185 °C to 182 °C and the following operating conditions C_{0Et}= 600 mg C/Nm^3, T_{1in}= 20 °C, F_{V0}= 61 m^3/h, Q_F= 600 W

The dynamic behaviour of the process for a subsequent negative step in $T_{0,SP}$ (from 182 to 179 °C) is shown in figure 8. The temporary profile of the reactor outlet temperature (T_e) is exhibited in Fig. 8a where an inverse response similar to that observed in Figure 7a is registered. However, its final steady-state is 7 °C lower than the initial one. This high decrease in T_e corresponds to lower VOCs conversion and consequently lower heat generation. In fact, the temporal profile of the outlet VOCs concentration (Figure 8c) exceeds the emission limit value (ELV = 20 mg C / Nm^3), indicating incomplete VOCs elimination when T_0 is not high enough.

To maintain the T_0 in the new setpoint value despite the lower heat generation at the reactor, the flow rate (λ = 0.638) through the FEHE has to be increased (see Figure 8b). Finally, although the control objective ($T_{0,\,SP}$ = 179 °C) is fulfilled, the process objective of ensuring the ELV is not accomplished.

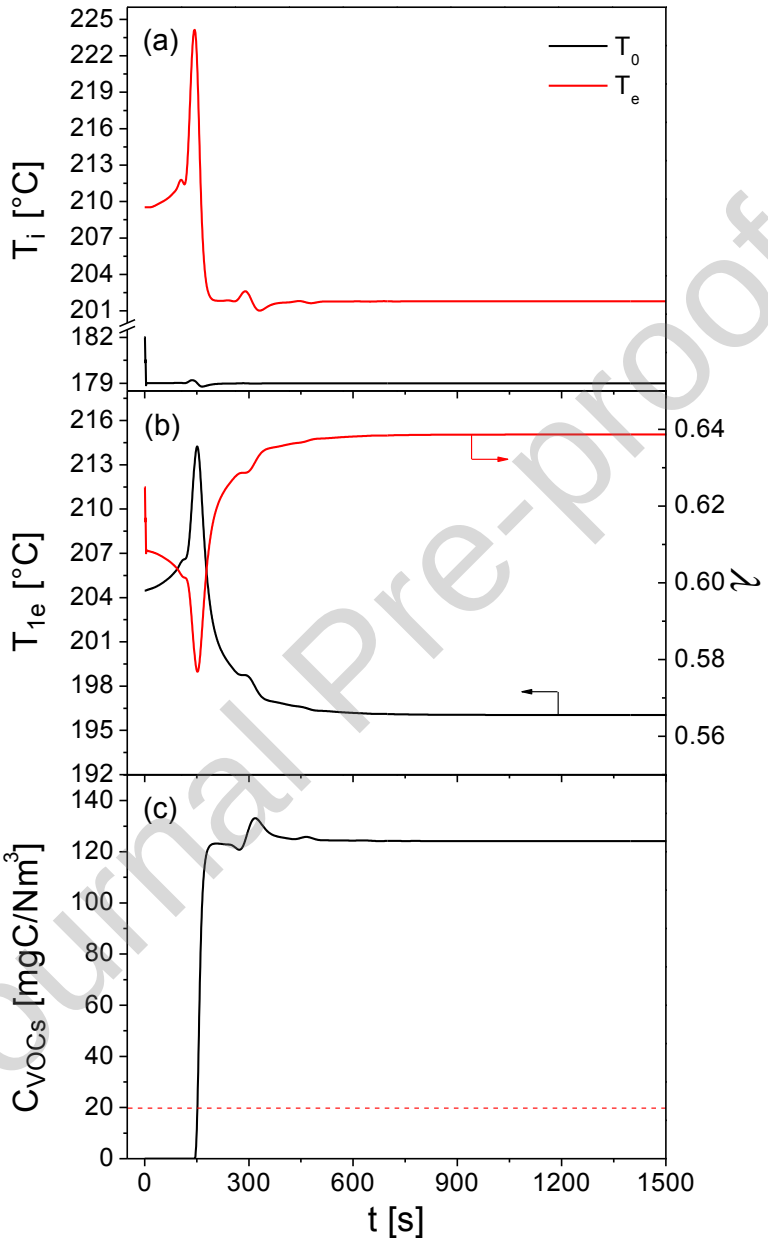

Fig. 8. (a) Temporary profiles of the reactor inlet and outlet temperatures, (b) Left ordinate axis: temporary profiles of the heat exchanger outlet temperature (T_{1e}), Right ordinate axis: temporary profile of the ratio of feed flow rate through FEHE, and (c) Temporary profiles of outlet VOCs concentrations, for a negative step in $T_{0,SP}$ from 182 °C to 179 °C, at the condition of Fig. 7.

3.2.2. Temporary VOC emission patterns

To analyse the effect of the temporary VOCs emission patterns over the process performance, three square pulses VOCs concentration disturbances (C_{0Et}) of different lengths are selected for a fixed heat supply from the furnace (Q_F).

Figure 9 a, b, c shows the three disturbances introduced in C_{0Et}. For this case, Q_F = 300 W and T_0= 185 °C are selected. The remaining conditions are listed in Table 3. The second row (Figures 9 d, e, f) shows the temporal profiles of T_0 and T_e for each case, and the third row (Figures 9 g, h, i) exhibits the corresponding outlet VOCs concentration in the left ordinate axis and the ratio of the flowrate through the FEHE (λ) in the right ordinate axis.

The temporary diminution of C_{0Et} from 600 to 300 mg C/Nm^3 in a square pulse pattern of 5 minutes of duration (Fig. 9a) leads to a decrease in the heat generation inside the reactor. With the aim of increasing the heat recovery through the FEHE, the bypass valve closing reaches its operative limit (plateau line at λ = 0.9) in two moments, first for 400 s (at t= 280 s) and then for 90 s (at t= 610 s).

During this time the process shows an oscillatory behaviour in T_0 and T_e, and also in λ (see Fig. 9d and 9g), due to the loss in the process controllability through the final control element. Despite the T_0 oscillatory profile, their values are high enough to guarantee the VOCs abatement, accomplishing the ELV. After the C_{0Et} value is restored over the 5 minutes, the reactor gradually recovers the initial heat generation condition, and λ returns to the initial steady-state value of 0.82.

In the next case, the temporary diminution of C_{0Et} from 600 to 300 mg C/Nm^3 in a square pulse pattern of 10 minutes of duration is shown in Fig. 9b. As before, the heat generation inside the reactor diminishes and the by-pass valve is operated to its limit for a longer time period (from t = 200 s to t= 2000 s). The heat recovered in the heat exchanger is not enough and T_0 and T_e show an oscillatory decrease. While T_0 is lower than $T_{0,SP}$ (from t= 50 s to t= 950 s), the process emits VOCs to the environment as Fig. 9h demonstrates. Notice that even though C_{0Et} is restored at t= 600 s, T_0 continues decreasing to t~ 950 s, due to the high time constant (τ_{HB}) of the reactor energy balance (see Eq. 7) (thermal inertia phenomena). After that, strong oscillations are observed in T_0 and T_e until the reactor heat generation is restored and consequently the by-pass valve controllability is recovered.

In the last case, the diminution of C_{0Et} from 600 to 300 mg C/Nm^3 in a square pulse of 15 minutes is simulated. Again, the low heat generation leads to a controllability loss in

the final control element. Unlike the previous cases, when C_{0Et} is restored to 600 mg C /Nm^3, the reactor inlet temperature is extremely low (T_0~ 162 °C), the reactions are extinguished and the loss of controllability is irreversible. Thus, the reactor and the FEHE temperatures tend to decrease toward the ambient temperature (T_{in}) as shown in Fig. 9f.

To avoid this undesirable situation a higher Q_F is required. For the next study cases, a Q_F= 600 W is selected.

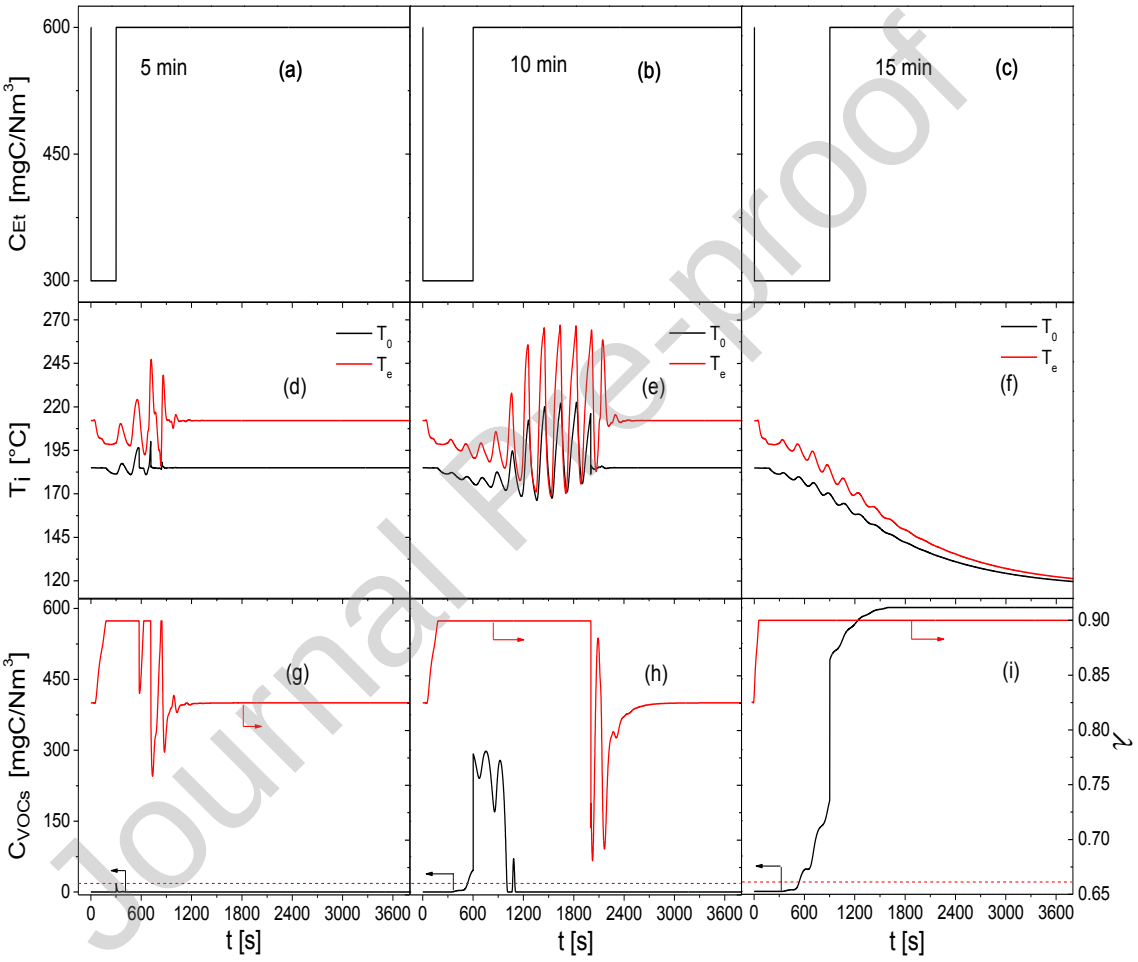

Fig. 9. (a,b,c) Square pulse patterns of inlet ethanol concentration (C_{0Et}). (d, e, f) Temporary profiles of reactor inlet and outlet temperatures. (g, h, i) Left ordinate axis: Temporary profile of VOCs concentration at $z = L$, Right ordinate axis: ratio of feed flow rate through FEHE (λ), for F_{V0}= 61 m^3/h, Q_F= 300 W, T_{1in}= 20 °C

Fig. 10 shows the dynamic response to a temporary diminution of C_{0Et} from 600 to 0 mg C/Nm^3 in a square pulse pattern of 15 minutes of duration. Due to the lack of heat generation inside the reactor, most of the feed stream goes through the heat exchanger

to maintain the T_0 in its reference value, which is achieved. Along this period of absence of VOCs, the temperature rise in the reactor vanishes. Thus, it can be observed in Fig. 10b that T_0 and T_e are equal during this time, which means that all the reactor length is at the same temperature (185 °C). Despite this, the process can operate under control. When the C_{0Et} is restored, the thermal profile inside the reactor is gradually recovered. For a short period of time (100 s) the outlet VOC concentration overpasses the ELV until the temperature inside the reactor sufficiently increases.

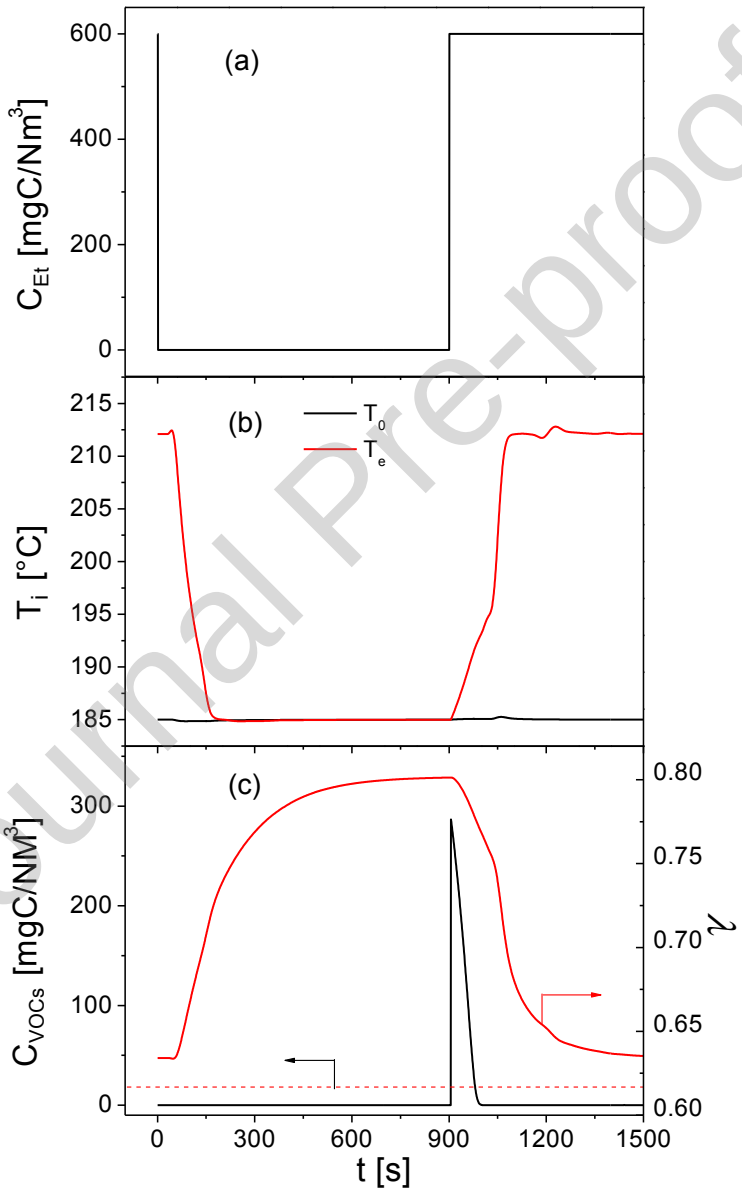

Fig. 10. (a) Square pulse pattern of inlet ethanol concentration, (b) Temporary profiles of the reactor inlet and outlet temperatures. (c) Left ordinate axis: Temporary profile of VOCs concentration at $z = L$, Right ordinate axis: ratio of feed flow rate through FEHE (λ), for F_{V0}= 61 m^3/h, T_{1in}= 20 °C, Q_F= 600 W.

Figure 11 shows the axial temperature profiles and total VOCs concentration profiles after VOCs feed concentration is restored, at times *t*=950, 975, 1000 and 1050 s.

The temperature profiles evolve in a rising thermal wave and recover the initial shape (t= 0s) at about 1200s. It is observed the ELV is accomplished before this time. Thus, for *t* =1000 s (100 s after C_{0Et} restored), the total VOCs are completely removed inside the reactor because the temperature is high enough.

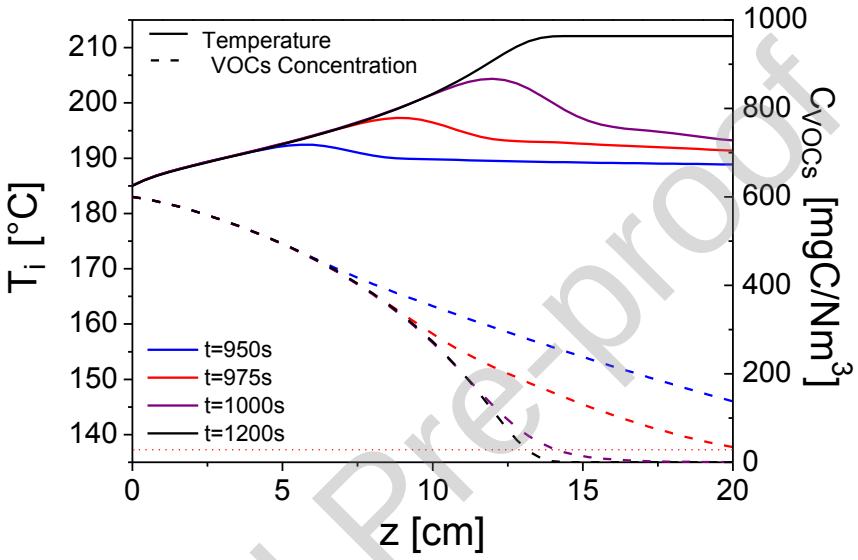

Fig. 11. Axial temperature and VOCs concentration profiles in the reactor for the conditions of Figure 10.

3.2.3. FEHE design considerations

In this section the influence of the heat exchanger area on the process behaviour is analysed. Figure 12 shows the temporary profiles of the main operating variables when a permanent diminution (negative step) in C_{0Et} from 600 to 400 mg C/Nm^3 occurs. The total heat exchange transfer area selected is 0.78 m^2.

In this situation, the final control element works at its operative maximum, redirecting almost the total feed stream to the heat exchanger (λ=0.9) with the aim of recovering the heat generated in the reactor (lower than the initial one). Despite this, the transfer area is not enough to recover the heat from the reactor outlet stream. As a consequence, T_{1e} decreases, thus T_0 tends to diminish leading to a gradually poorer VOCs conversion inside the reactor and finally, with the extinction of the reactions, the VOCs leave the

reactor unconverted as shown in Fig. 12b, the inlet reactor VOC concentration and outlet reactor VOCs concentration (at z=20cm) are equal.

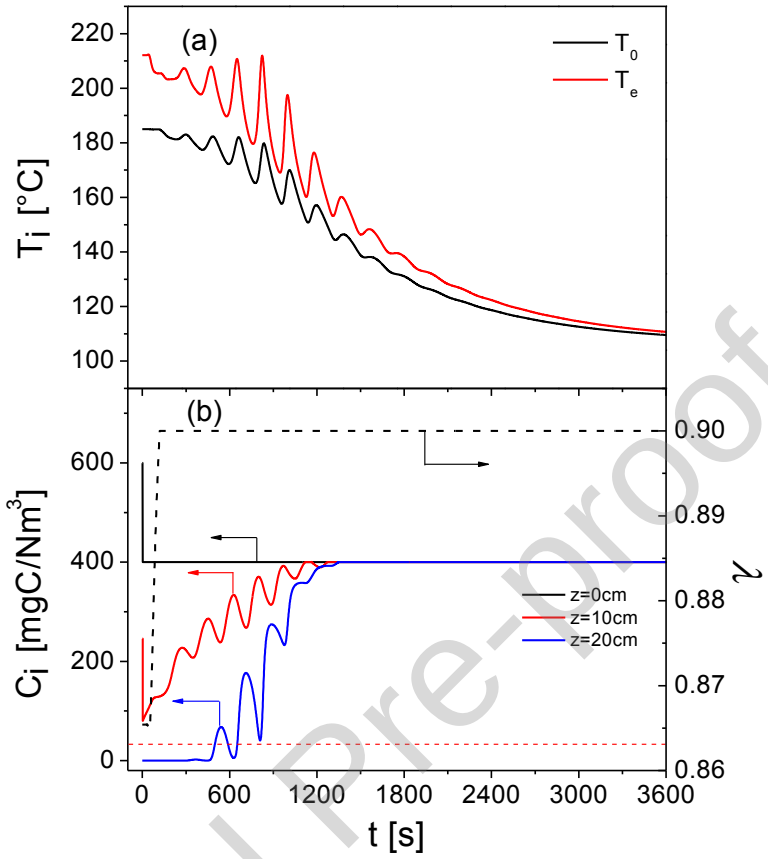

Fig. 12. (a) Temporary profiles of inlet and outlet reactor temperatures. (b) Left ordinate axis: Temporary profile of VOCs concentration at different reactor axial positions, Right ordinate axis: ratio of feed flow rate through FEHE (λ), for a FEHE transfer area A_T = 0.78 m^2, F_{v0}= 61 m^3/h, T_{1in}= 20 °C, Q_F= 300 W.

Figure 13 shows the dynamic performance of the process for a negative step in C_{0Et} from 600 to 400 mg C/Nm^3, with a heat exchange transfer area of 0.9 m^2, higher than the previous case.

Under this situation, the by-pass valve works almost completely closed (λ = 0.9). The loss of controllability on the by-pass valve turns the system unstable, then a sustained oscillatory behaviour is observed in state variables as T_0, T_e, and VOCs concentration inside the reactor. That shows that limit cycles can not only appear in open-loop operation, but also in closed-loop operation, when the final action element is saturated.

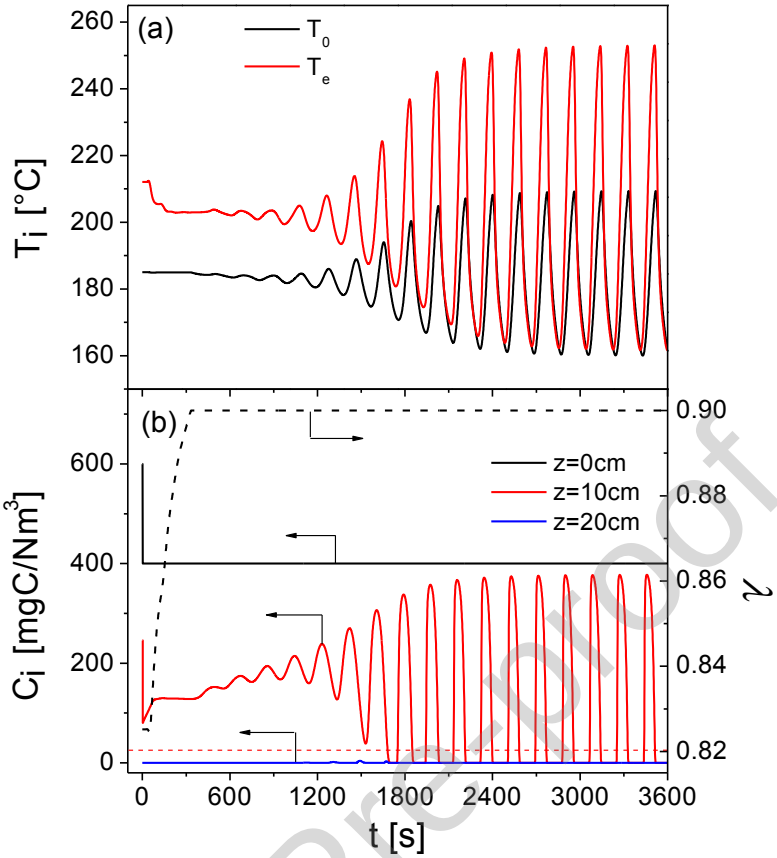

Fig. 13. (a) Temporary profiles of inlet and outlet reactor temperatures. (b) Left ordinate axis: Temporary profile of VOCs concentration at different reactor axial positions, Right ordinate axis: ratio of feed flow rate through FEHE (λ), for a FEHE transfer area A_T =0.90 m^2, F_{v0}= 61 m^3/h, T_{1in}= 20 °C, Q_F= 300 W.

Figure 14 shows the effect of increasing the heat exchanger transfer area. In this case, an A_T= 1.12 m^2 is selected. As expected, when the inlet VOC concentration diminishes (from 600 to 400 mg C/Nm^3), the heat generation in the reactor decreases, and consequently T_e (see Figure 14a). A higher ratio of the feed stream is conducted through the FEHE. Notice that in this case, the by-pass valve does not work in its operative limit due to an expansion in the controllability range of the by-pass valve caused by the increase in the heat exchange area. A high enough transfer area allows efficient heat recovery from the reactor outlet stream, and it is possible to maintain the inlet temperature at its reference value, $T_{0,SP}$ to perform an efficient VOC elimination.

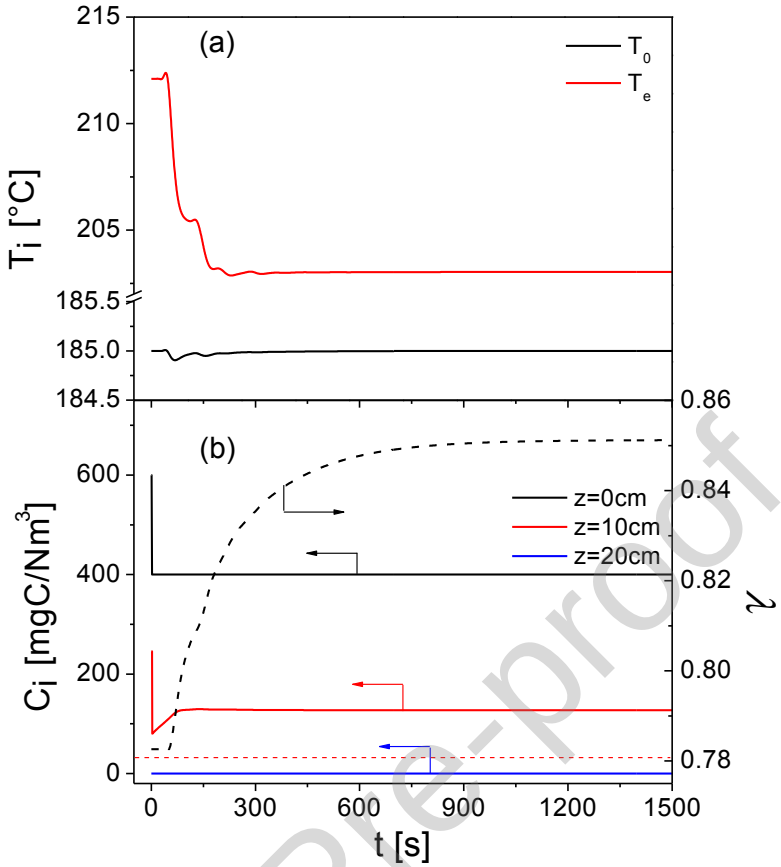

Fig. 14. (a) Temporary profiles of inlet and outlet reactor temperatures. (b) Left ordinate axis: Temporary profile of VOCs concentration at different reactor axial positions, Right ordinate axis: ratio of feed flow rate through FEHE (λ), for a FEHE transfer area A_T = 1.12 m^2, F_{v0}= 61 m^3/h, T_{1in}= 20 °C, Q_F= 300 W.

4. Conclusions

Under open-loop conditions, the catalytic combustion process presents an inherent instability related to the positive feedback of the heat recovered in the heat exchanger (FEHE) leading to pronounced limit cycles in the main state variables (reactor and FEHE temperatures and VOCs concentration along the reactor). The heat supplied by the furnace provides a clear stabilizer effect. As the furnace heat supply increases (lower heat recovery in the FEHE), the limit cycles appear later and show gradually lower amplitude.

A single-loop feedback control system is successfully applied to maintain the inlet temperature set-point by manipulating the by-pass valve around the FEHE. The proposed control structure enables the system to reject severe disturbances in the feed

concentration of VOCs. Provided that the bypass valve operates far from its saturation point, stable conditions can be guaranteed.

The heat exchanger area plays a key role and must be carefully defined. Higher FEHE heat-transfer areas expand the controllability range of the by-pass valve leading to a more efficient heat recovery. This positive effect must be weighed against the increase in investment cost.

Acknowledgements

The authors acknowledge the support of the National University of San Luis, the National University of the South, the National Agency for Scientific and Technical Promotion (ANPCyT) and the National Scientific and Technical Research Council (CONICET).

References

[1] R.M. Heck, R.J. Farrauto, S. Gulati, Catalytic Air Pollution Control, Commercial Tech. Wiley, NY, USA (2002), https://doi.org/10.1002/ep.670210408.

[2] F. Wu, Y. Lu, M. Wang, X. Zhang, C. Yang, Catalytic Removal of Ozone by Pd/ACFs and Optimal Design of Ozone Converter for Air Purification in Aircraft Cabin, Civil Engineering Journal, 5 (2019) 1656-1671. https://doi.org/10.28991/cej-2019-03091361

[3] E. Tronconi, L. Lietti, P. Forzatti, S. Malloggi, Experimental and theoretical investigation of the dynamics of the SCR - DeNOx reaction, Chemical Engineering Science, 51 (1996) 2965-2970, https://doi.org/10.1016/0009-2509(96)00182-0

[4] X. Wang, R. Daniels, R.W. Baker, Recovery of VOCs from high-volume, low VOC-concentration air streams, AIChE J. 47 (2001) 1094-1100, https://doi.org/10.1002/aic.690470516.

[5] Z. Zhangab Z. Jiangc W. Shangguan. Low-temperature catalysis for VOCs removal in technology and application: A state-of-the-art review. Catalysis Today V. 264 (2016) 270-278, https://doi.org/10.1016/j.cattod.2015.10.040.

[6] European Union Law. https://eur-lex.europa.eu/legal-content/EN/TXT/?uri=LEGISSUM%3Al28029b. (Last accessed 24/03/21)

[7] J. Yang; Y. Chen; L. Cao; Y. Guo; J. Jia, Development and field-scale optimization of a honey combzeolite rotor concentrator/recuperative oxidizer for the abatement of

volatile organic carbons from semiconductor industry, Environ. Sci. Technol. 46 (2012) 441–446, https://doi.org/10.1021/es203174y.

[8] P. Marín; F. Diez; S. Ordoñez, A new method for controlling the ignition state of a regenerative combustor using a heat storage device, Appl. Energy 116 (2014) 322–332, https://doi.org/10.1016/j.apenergy.2013.11.070.

[9] William L. Luyben. New Control Structure for Feed-Effluent Heat Exchanger/Reactor Systems. Ind. Eng. Chem. Res. 51, 25 (2012) 8566–8574, https://doi.org/10.1021/ie3004896.

[10] Jogwar, S. S.; Baldea, M.; Daoutidis, P. Dynamics and Control of Reactor – Feed Effluent Heat Exchanger Networks, Proceedings of the American Control Conference, (2008) 1481-1486, https://doi.org/10.1109/ACC.2008.4586701.

[11] Bildea, C. S.; Dimian, A. C. Stability and multiplicity approach to the design of heat-integrated PFR. AIChE J. 44 (1998) 2703−2712, https://doi.org/10.1002/aic.690441211.

[12] Morud, J. C.; Skogestad, S. Analysis of instability in an industrial ammonia reactor. AIChE J. 44 (1998) 888−895, https://doi.org/10.1002/aic.690440414.

[13] Silverstein, J. L.; Shinnar, R. Effect of design on the stability and control of fixed bed catalytic reactors with heat feedback: 1. Concepts. Ind. Eng. Chem. Process Des. Dev. 21 (1982) 241−256, https://doi.org/10.1021/i200017a007.

[14] Terrill, D. L.; Douglas, J. M. Heat-exchanger network analysis: 2 Steady-state operability evaluation. Ind. Eng. Chem. Res. 26 (1987) 691-696, https://doi.org /10.1021/ie00064a011.

[15] M. L. Rodriguez, L. Cadus , D. Borio, Effect of Heat Losses on Monolithic Reactors for VOC Abatement, Chemical Engineering Journal, 377 (2019), https://doi.org/10.1016/j.cej.2018.10.076.

[16] J. Zhen, Y. Yu, Z. Zhang, X. Wang, S. Yin, K. Peng, X. Feng, H. Cai, Industrial sector-based volatile organic compound (VOC) source profiles measured in manufacturing facilities in the Pearl River Delta, China, (2013), 456-457, https://doi.org/10.1016/j.scitotenv.2013.03.055.

[17] Luyben, W. L.; Tyreus, B. D.; Luyben, M. L. Plantwide Process Control (1998), 167, ISBN: 0070067791.

[18] W. L. Luyben, Control Structures for Process Piping Systems, Chemical Engineering Research and Design, (2020), 162, https://doi.org/10.1016/j.cherd.2020.07.022.

[19] M. R. Morales, B. Barbero, L. E. Cadús, Total oxidation of ethanol and propane over Mn-Cu mixed oxide catalysts, Applied Catalysis B Environmental 67 (2006), 229-236, https://doi.org/10.1016/j.apcatb.2006.05.006.

[20] M.A. Campesi, J. Mariani, M. C. Pramparo, B. Barbero, L. E.Cadús, O. M. Martínez G. F. Barreto, Combustion of volatile organic compounds on a MnCu catalyst: A kinetic study, Catalysis Today, 176 (2011), 225-228, https://doi.org/10.1016/ j.cattod.2011.01.009.

[21] A.F. Miranda, M.L. Rodriguez, D. Borio, Obtaining effective reaction rates in monolithic reactors for ethanol combustion. (Spanish language), IV RITeQ, Carlos Paz, Córdoba, Junio (2018).https://drive.google.com/file/d/17HuZ89LsrHVHZIiFIn7hNXd Z9bnuCMo3/view .

[22] A. Cybulski, J.A. Moulijn, Monoliths in heterogeneous catalysis, Catal. Rev. 36 (1994) 179–270, https://doi.org/10.1080/01614949408013925.

[23] J.M. Smith, H.C. Van Ness, M.M. Abbott, Introduction to Chemical Engineering Thermodynamics, McGraw-Hill, New York, 2005.

[24] Shampine, C.W. Gear, A users view of solving stiff ordinary differential equations, SIAM Rev. 21 (1979) 1–17. https://doi.org/10.1137/1021001.

[25] J. A. Hoiberg, B. C. Lyche, A. S. Foss, Experimental Evaluation of Dynamic Models for a Fixed-Bed Catalytic Reactor, AlChE Journal, 17 (1971), 1434-1447, https://doi.org/10.1002/aic.690170627.

Nomenclature

A_f'	FEHE transversal flow area, m^2
$A´$	Heat exchanger surface area, m^2
A_s	Cordierite surface area, m^2
A_w	Washcoat surface area, m^2
A_t	Reactor surface area, m^2
b	Channel width=height, mm
$b´$	FEHE plate width, m
C_j	Concentration of j component, mol_j/m^3 or mg C/ Nm^3
$\overline{Cp}_k$	Average heat capacity of k stream in the heat exchanger, J/mol_j K

CN	Channel number, dimensionless
er	Deviation between set point value and controlled variable
E_i	Activation energy of *i* reaction, J/mol
ELV	Emission Limit Value, 20 mg C/Nm^3 (total VOC emissions at standard conditions)
F_V	Volumetric feed flow rate, Nm^3 /h
$GHSV$	Gas-Hourly space velocity, 1/h
h_i	convective heat transfer coefficient, J/ (s m^2 K)
HD	Hydraulic diameter, m
$k_{\cdot}$	Thermal conductivity of heat exchanger material, J/ (s m K)
k_k	Thermal conductivity of *k* stream in FEHE, J/ (s m K)
$k_{ref,1}$	Kinetic constant of reaction 1, 1/s
$k_{ref,2}$	Kinetic constant of reaction 2, mol/(m^3 s)
K_c	Proportional action parameter
k_{cj}	Adsorption constant of j component, m^3/mol
L	Reactor channel length, m
$L^{\prime}$	Heat exchanger length, m
$\dot{m}$	Total mass flow, kg/s
m_s	Cordierite mass, g
m_w	Catalyst mass, g
Nu_k	Nusselt number of *k* FEHE stream, dimensionless
P	Pressure, kPa
PN	Plates number, dimensionless
Pr	Prandtl number, dimensionless
Q_F	Furnace heat supply, W
Q_R	Heat recovered by FEHE, W
Q_{tot}	Total heat to preheat the feed, W
r_i	Reaction rate of i reaction, mol/(m$_g^3$s)
Re	Reynold number, dimensionless
t	Time, s
T	Reactor temperature, °C
T_e	Reactor outlet temperature= Hot stream inlet temperature (FEHE), °C

T_k	Temperature of *k* FEHE stream, °C
U	Global heat transfer coefficient, W/(m^{2}K)
u_s	Gas reactor velocity, m/s
u_k	Gas velocity of *k* FEHE stream, m/s
V1	By-pass valve
V2	Downstream FEHE valve
z	Reactor axial coordinate, m
z'	Heat exchanger axial coordinate, m

Compounds / acronyms

LHHW	Langmuir-Hinshelwood Hougen-Watson
NOx	Nitrogen oxides
VOC	Volatile Organic Compound

Greek letter

δ'	Plate thickness, mm
δ_w	Washcoat thickness, µm
ρ_w	Washcoat density, kg/m^3
$\Delta H_{ri°}$	Heat of i reaction at standard conditions, J/mol
ΔH_{ri}	Heat of i reaction, J/mol
ΔT_{ad}	Adiabatic temperature gradient, K
ΔT_F	Temperature rise caused by the furnace
ΔC_{0Et}	Concentration disturbance, mg C/Nm^3
ε_{1r}	Degree of advancement of reaction 1
ε_{2r}	Degree of advancement of reaction 2
ε	Reactor porosity
$\overline{\rho}_i$	Gas density of *i* stream in FEHE, kg/m^3
$\wp_w$	Washcoat density, kg/m^3
λ	fraction of stream through the FEHE
$1-\lambda$	fraction of stream through bypass
τ_I	integral action parameter (or integral time)
τ	time constant, m/s

Subscripts

Ac	Acetaldehyde
e	Exit
Et	Ethanol
g	Reactor gas stream
HE	Heat exchanger balance
i	reaction
j	component
k	FEHE stream (cold stream: 1, hot stream: 2)
mix	Mixer point
MB	Reactor mass balance
ref	Reference
s	Cordierite (substrate)
SP	Set point
VOC	Volatile organic compound
w	Washcoat
0	At the axial coordinate z=0
1	FEHE cold stream
2	FEHE hot stream

Superscripts

SS	Steady state
eff	observable expressions of rate

Author Statement

Ángel Federico Miranda: Software, Formal analysis, Investigation, Writing - Original Draft Preparation, Visualization

María L. Rodríguez: Conceptualization, Methodology, Resources, Writing - Review & Editing

Luis E. Cadús: Conceptualization

Daniel O. Borio: Conceptualization, Resources, Writing - Review & Editing, Supervision

Declaration of interests

☒ The authors declare that they have no known competing financial interests or personal relationships that could have appeared to influence the work reported in this paper.

☐The authors declare the following financial interests/personal relationships which may be considered as potential competing interests:

Highlights

- Dynamic study of a FEHE/Reactor system for catalytic combustion of VOCs is performed.
- The feedback of energy to the feed stream produces instability and limit cycles
- Influence of variable emission patterns on process stability is analysed.
- There is a compromise between the external energy supply and stability.
- Limit cycles appear in closed-loop operation when the by-pass valve is saturated
- Low heat exchanger areas lead to by-pass valve saturation and instability.